

Dalton Transactions

Accepted Manuscript



This is an *Accepted Manuscript*, which has been through the Royal Society of Chemistry peer review process and has been accepted for publication.

Accepted Manuscripts are published online shortly after acceptance, before technical editing, formatting and proof reading. Using this free service, authors can make their results available to the community, in citable form, before we publish the edited article. We will replace this *Accepted Manuscript* with the edited and formatted *Advance Article* as soon as it is available.

You can find more information about *Accepted Manuscripts* in the [Information for Authors](#).

Please note that technical editing may introduce minor changes to the text and/or graphics, which may alter content. The journal's standard [Terms & Conditions](#) and the [Ethical guidelines](#) still apply. In no event shall the Royal Society of Chemistry be held responsible for any errors or omissions in this *Accepted Manuscript* or any consequences arising from the use of any information it contains.

Two Novel Thioarsenates $\{[\text{Mn}(2,2'\text{-bipy})_2(\text{SCN})][\text{Mn}(2,2'\text{-bipy})](\text{As}^{\text{V}}\text{S}_4)\}_2$ and $\{[\text{Mn}(2,2'\text{-bipy})_2(\text{SCN})]_2[\text{As}^{\text{III}}_2(\text{S}_2)_2\text{S}_2]\}$: Introducing an Anionic Second ligand to Modify Mn^{II} Complex Cations of 2,2'-Bipyridine

Guang-Ning Liu,^{a,b} Guo-Cong Guo,^{b,*} Ming-Sheng Wang,^b and Jin-Shun Huang^b

a Key Laboratory of Chemical Sensing & Analysis in Universities of Shandong, School of Chemistry and Chemical Engineering, University of Jinan, Jinan, Shandong 250022, P. R. China.

b State Key Laboratory of Structural Chemistry, Fujian Institute of Research on the Structure of Matter, Chinese Academy of Sciences, Fuzhou, Fujian 350002, P. R. China. E-mail: gcguo@fjirsm.ac.cn

Abstract

Two novel manganese thioarsenates, $\{[\text{Mn}(2,2'\text{-bipy})_2(\text{SCN})][\text{Mn}(2,2'\text{-bipy})](\text{As}^{\text{V}}\text{S}_4)\}_2$ (**1**, 2,2'-bipy = 2,2'-bipyridine) and $\{[\text{Mn}(2,2'\text{-bipy})_2(\text{SCN})]_2[\text{As}^{\text{III}}_2(\text{S}_2)_2\text{S}_2]\}$ (**2**) containing thiocyanate-modified Mn-2,2'-bipy (2,2'-bipy = 2,2'-bipyridine) complex cations were synthesized. They feature two terminal $[\text{Mn}(2,2'\text{-bipy})_2(\text{SCN})]^+$ complex cations bridged by a polyanion $\{[\text{Mn}(2,2'\text{-bipy})]_2(\text{As}^{\text{V}}\text{S}_4)_2\}^{2-}$ for **1** and a cyclic thioarsenate anion $(\text{As}^{\text{III}}_2\text{S}_6)^{2-}$ for **2**. In **2**, the $[\text{As}^{\text{III}}_2(\text{S}_2)_2\text{S}_2]^{2-}$ anion can be described as two $(\text{As}^{\text{III}}\text{S}_3)^{3-}$ trigonal-pyramids interlinked through S–S bonds. The method to get new metal complex cations shown here, introducing an anionic second ligand to modify the number of the coordination sites and the charges of the metal complex cations simultaneously, is different from the traditional methods, varying either the TM center or the organic ligand or employing mixed neutral organic ligands, and may open up a new route for preparing novel chalcogenidometalates. Compounds **1** and **2** exhibit wide optical gaps of 2.20 and 2.67 eV, respectively, and photoluminescence with the emission maxima occurring around 440 nm. Magnetic measurements show the presence of antiferromagnetic interactions between Mn^{II} centers in the two compounds.

Keywords: Anionic second ligand; Inorganic-Organic Hybrid; Magnetism; Photoluminescence; Thioarsenates.

1. Introduction

During the past several years, main-group element chalcogenide-based materials have attracted continuing interest due to their fascinating structural features and potential applications in nonlinear optics, ion exchange, storage materials, photocatalysis, electro-optics and fast-ion conductivity.¹ Among these materials, those formed by incorporating unsaturated transition-metal (TM) or rare-earth-metal (Ln) complex cations² into the inorganic main-group element chalcogenide framework have received more attention because it can generate unique topological structures and interesting properties.^{1a-d,3} It has been demonstrated that the unsaturated TM or Ln complex cations with different size, shape, charge as well as the number of the coordination sites left for coordinating with chalcogenide anion can significantly influence the inorganic main-group element chalcogenide anionic frameworks.^{1a-d,4} Accordingly, try the best to get novel unsaturated metal complex cations, is a key point in the synthesis of new chalcogenidometalates. Previous studies in obtaining diverse unsaturated metal complex cations are mainly concentrated on varying the metal center or the organic ligand, or employing mixed neutral organic ligands.^{3d,4b,5} The introduction of an anionic second ligand, which will modify the number of the coordination sites for chalcogenide anion and the charges of the unsaturated metal complex cations simultaneously, is very attractive, but has not been performed in the syntheses of hybrid main-group element-based chalcogenides.

In this work, we select SCN^- anion as an anionic second ligand to modify metal complex cations with the aim to synthesize new chalcogenidometalates. Successfully, two novel manganese thioarsenates with *in-situ* formed $\text{Mn}^{\text{II}}\text{-2,2'}$ -bipy- SCN^- complex cations were isolated, namely, $\{[\text{Mn}(2,2'\text{-bipy})_2(\text{SCN})][\text{Mn}(2,2'\text{-bipy})](\text{As}^{\text{V}}\text{S}_4)\}_2$ (**1**), $\{[\text{Mn}(2,2'\text{-bipy})_2(\text{SCN})]_2(\text{As}^{\text{III}}_2\text{S}_6)\}$ (**2**) (2,2'-bipy = 2,2'-bipyridine). Herein, we report the syntheses, structures, optical and magnetic properties of **1** and **2**.

2. Experimental Section

2.1 Materials and Instruments.

All reagents were purchased commercially and used without further purification.

Elemental analyses of C, H, and N were performed on an Elementar Vario EL III microanalyzer. Powder X-ray diffraction (PXRD) patterns were recorded on Rigaku MiniFlex II diffractometer using Cu $K\alpha$ radiation. A NETZSCH STA 449C thermogravimetric analyzer was used to obtain TGA curves in N₂ with a flow rate of 20 mL/min and a ramp rate of 10 °C·min⁻¹ in the temperature range 30–1000 °C. An empty Al₂O₃ crucible was used as the reference. The FT-IR spectra were obtained on a Perkin-Elmer spectrophotometer using KBr disk in the range 4000–400 cm⁻¹. The solid-state fluorescence excitation and emission spectra were measured on an Edinberg EI920 fluorescence spectrophotometer at room temperature with a wavelength increment of 1.0 nm and an integration time of 0.2 s. Optical diffuse reflectance spectra were measured at room temperature with a PE Lambda 900 UV-vis spectrophotometer. The instrument was equipped with an integrating sphere and controlled with a personal computer. The samples were ground into fine powder and pressed onto a thin glass slide holder. A BaSO₄ plate was used as a standard (100% reflectance). The absorption spectra were calculated from reflectance spectrum using the Kubelka-Munk function:⁶ $\alpha/S = (1-R)^2/2R$ where α is the absorption coefficient, S is the scattering coefficient (which is practically wavelength independent when the particle size is larger than 5 μm), and R is the reflectance. The polycrystalline magnetic study was performed on a Quantum Design MPMS-XL SQUID magnetometer. All data were corrected for diamagnetism estimated from Pascal's constants.

2.2 Preparation for 1.

A mixture of As (0.038 g, 0.51 mmol), MnCO₃ (0.058 g, 0.50 mmol), S (0.064 g, 2.00 mmol), NH₄SCN (0.038 g, 0.50 mmol), and 2,2'-bipy (0.078 g, 0.50 mmol) in 5 mL distilled water was sealed in a 25-mL poly(tetrafluoroethylene)-lined stainless steel container under autogenous pressure and then heated at 150 °C for 5 days and finally cooled to room temperature. The product consists of orange prismatic crystals of **1** and a few bits of unidentified powder. The crystals of **1** were selected by hand and washed with ethanol and diethyl ether. (Yield: 7% based on As). The crystals are stable in air and insoluble in common solvents, and the phase purity of the hand-picked single crystals is confirmed by a PXRD study (Figure S1). Elemental analysis calcd. (%) for C₆₂H₄₈As₂Mn₄N₁₄S₁₀: C 44.34, H 2.88, N

11.68; found: C 43.13, H 2.67, N 11.22.

2.3 Preparation for **2**.

A mixture of As (0.075 g, 1.00 mmol), MnCO₃ (0.058 g, 0.50 mmol), S (0.160 g, 5.00 mmol), NH₄SCN (0.076 g, 1.00 mmol), and 2,2'-bipy (0.156 g, 1.00 mmol) in 5 mL distilled water was sealed in a 25-mL poly(tetrafluoroethylene)-lined stainless steel container under autogenous pressure and then heated at 150 °C for 6 days and finally cooled to room temperature. The product consists of light-yellow chunk crystals of **2** and a few bits of unidentified powder. The crystals of **2** were selected by hand and washed with ethanol and diethyl ether. (Yield: 15% based on As). The crystals are stable in air and insoluble in common solvents, and the phase purity of the hand-picked single crystals is confirmed by a PXRD study (Figure S1). Elemental analysis calcd. (%) for C₄₂H₃₂As₂Mn₂N₁₀S₈: C 42.29, H 2.70, N 11.74; found: C 41.95, H 2.59, N 11.79.

2.4 Single-Crystal Structure Determination.

The intensity data sets were collected on a Rigaku AFC7R diffractometer equipped with graphite-monochromated Mo *K*α radiation ($\lambda = 0.71073 \text{ \AA}$) using ω -2 θ scan technique at 293 K. The data sets were reduced by the CrystalStructure program.⁷ An empirical absorption correction was applied using ψ -scan method. The structures were solved by direct methods using the Siemens SHELXL package of crystallographic software.⁸ The difference Fourier maps created on the basis of these atomic positions to yield the other non-hydrogen atoms. The structures were refined using a full-matrix least-squares refinement on F^2 . All non-hydrogen atoms were refined anisotropically. The hydrogen atoms of 2,2'-bipy ligand were added geometrically and refined as riding on their parent atoms with fixed isotropic displacement parameters [$U_{\text{iso}}(\text{H}) = 1.2U_{\text{eq}}(\text{C}, \text{N})$]. There is an alert C “Structure contains solvent accessible voids of 44 Å³” in the checkcif file. The structure maybe a hydrate, crystallized from water, and has largely lost the water molecules prior to X-ray measurement. Application of procedure SQUEEZE (program PLATON) did not bring about a significant improvement of refinement results and therefore was not retained for the final refinement. The compound is therefore considered as a desolvate with no solvent content given in

chemical formula and quantities derived thereof. Crystallographic data and structural refinements for **1** and **2** are summarized in Table 1. Important bond lengths and angles are listed in Table S1.

Table 1. Crystal and Structure Refinement Data for **1** and **2**.

	1	2
Formula	C ₆₂ H ₄₈ As ₂ Mn ₄ N ₁₄ S ₁₀	C ₄₂ H ₃₂ As ₂ Mn ₂ N ₁₀ S ₈
M_r (g mol ⁻¹)	1679.34	1192.98
Crystal system	Triclinic	Triclinic
Space group	<i>P</i> -1	<i>P</i> -1
ρ_{calcd} [g cm ⁻³]	1.636	1.676
a [Å]	8.891(1)	8.770(1)
b [Å]	10.684(2)	10.034(1)
c [Å]	19.448(3)	13.597(2)
α [°]	77.252(13)	81.461(10)
β [°]	86.528(13)	89.595(11)
γ [°]	71.081(12)	87.716(11)
V [Å ³]	1704.5(5)	1182.3(3)
Z	1	1
T [K]	293(2)	293(2)
$F(000)$	844	598
θ range [°]	2.06–25.50	2.32–25.50
Measured reflections	6868	4764
Independent reflections (R_{int})	6328 (0.0432)	4391 (0.0230)
Data/params/restraints	4250/415/0	3010/289/0
R_1^a, wR_2^b [$I > 2\sigma(I)$]	0.0626, 0.1416	0.0478, 0.1080
R_1^a, wR_2^b (all data)	0.1147, 0.1853	0.0702, 0.1132
Goodness of fit	1.004	1.008
$\Delta\rho_{\text{max}}$ and $\Delta\rho_{\text{min}}$ [e Å ⁻³]	1.131, -0.950	1.104, -1.185
^a $R_1 = \sum F_o - F_c / \sum F_o $, ^b $wR_2 = \{\sum w[(F_o)^2 - (F_c)^2]^2 / \sum w[(F_o)^2]\}^{1/2}$		

3. Results and Discussion

3.1 Synthetic Considerations.

It should be mentioned that compounds **1–2** are gained in relatively low yields (7% and 15%, respectively) despite a broad variation of the synthesis conditions. The described synthesis methods are the best ones to yield the title compounds up to now and the reproducibility of all the products are good. Compounds **1–2** are well isolated with distilled water used as solvent; further experiments with methylamine aqueous solutions instead of distilled water are fruitless. MnCO_3 used in the syntheses of **1–2** is perfect as the Mn^{2+} resource material in our experiments. Detailed experiments show that compounds **1–2** still can be formed in a lower yield when MnCO_3 is replaced by $\text{MnCl}_2 \cdot 4\text{H}_2\text{O}$. The described stoichiometry of the reactant in the text is perfect for the preparation of the title compounds.

3.2 Crystal Structures.

Compounds **1** and **2** feature a similar centrosymmetric molecular structure, which contains two terminal $[\text{Mn}(2,2'\text{-bipy})_2(\text{SCN})]^+$ complex cations bridged by a polyanion $\{[\text{Mn}(2,2'\text{-bipy})]_2(\text{As}^{\text{V}}\text{S}_4)_2\}^{2-}$ for **1** and a cyclic thioarsenate anion $(\text{As}^{\text{III}}_2\text{S}_6)^{2-}$ for **2** (Figures 1 and 2). The local coordination geometry around each Mn center in the terminal $[\text{Mn}(2,2'\text{-bipy})_2(\text{SCN})]^+$ complex cations of both compounds can be best described as a distorted octahedron involving five N atoms from two chelating 2,2'-bipy ligands and one terminal SCN^- ligand, and one S atom from the bridging anion. The serious distortions of the (MnN_5S) octahedra are reflected in the axial *trans* bond angles deviating from 180° (Table S1). It should be noted that the SCN^- groups in **1** and **2** are almost linear with N–C–S bond angles of $178.7(3)^\circ$ and behave as a N-donor ligand coordinating to the Mn^{2+} ion in the terminal complex cations in a linear fashion with Mn–N–C bond angles of $166.86(32)$ and $173.14(29)^\circ$ for **1** and **2**, respectively.

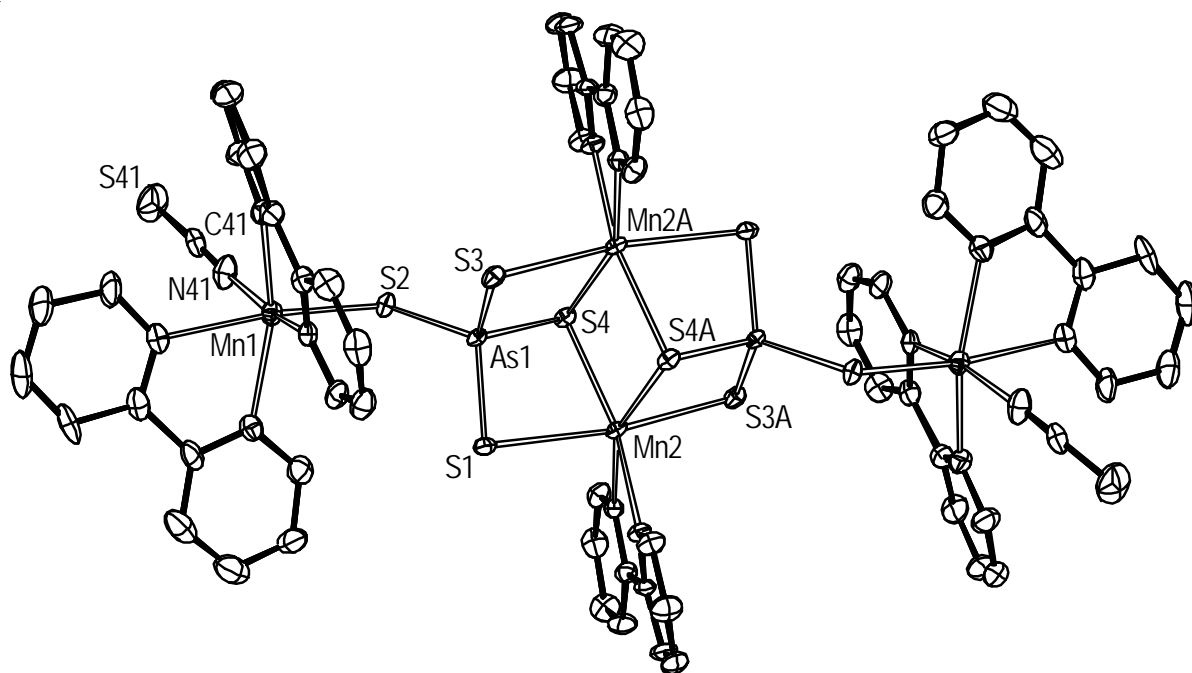


Figure 1. ORTEP drawing of **1** with 30% thermal ellipsoids and hydrogen atoms being omitted for clarity. Symmetry code: A (1-x, 1-y, 1-z).

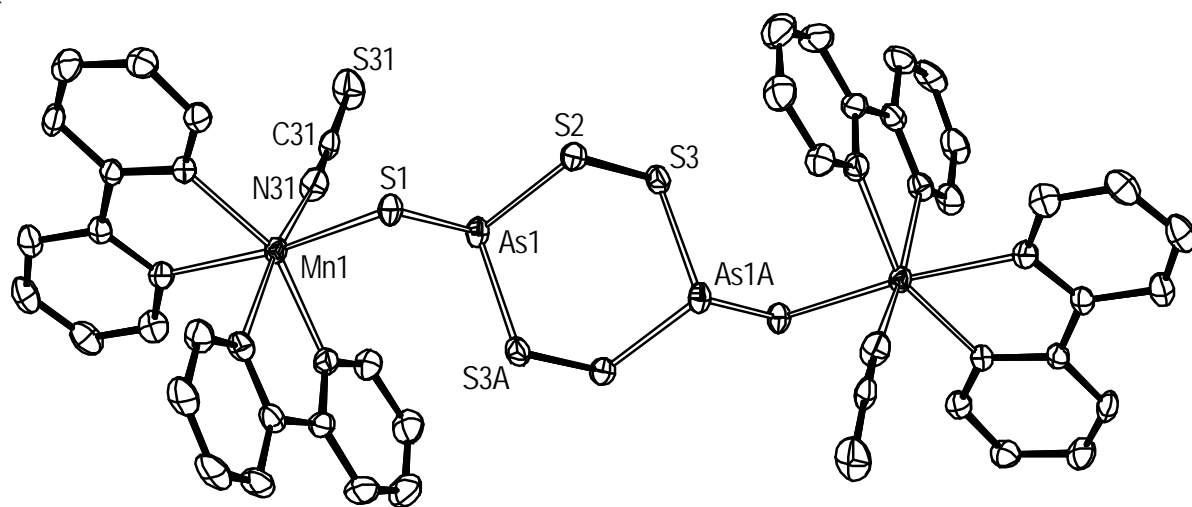


Figure 2. ORTEP drawing of **2** with 30% thermal ellipsoids and hydrogen atoms being omitted for clarity. Symmetry code: A (1-x, 2-y, 1-z).

In **1**, the bridging polyanion $\{[\text{Mn}(2,2'\text{-bipy})]_2(\text{As}^{\text{V}}\text{S}_4)_2\}^{2-}$ with a crystallographically imposed center of symmetry is established by the connection of two symmetry-related $[\text{Mn}(2,2'\text{-bipy})]^{2+}$ fragments and two symmetry-related $(\text{As}^{\text{V}}\text{S}_4)^{3-}$ anions (Figure 1). Each As atom is coordinated by three μ_2 - and one μ_3 -S atoms to form a slightly distorted $(\text{As}^{\text{V}}\text{S}_4)^{3-}$

tetrahedron, which acts as a μ_3 -(As^VS₄)³⁻ ligand connecting two symmetry-related [Mn(2,2'-bipy)]²⁺ and one terminal [Mn(2,2'-bipy)₂(SCN)]⁺ fragments with the Mn...Mn distances of 7.084(1), 6.798(1) and 3.769(1) Å for Mn1...Mn2, Mn1...Mn2A and Mn2...Mn2A, respectively. The Mn²⁺ ions in the two [Mn(2,2'-bipy)₂(SCN)]⁺ complex cations are well separated by the bridging cluster, {[Mn(2,2'-bipy)]₂(As^VS₄)₂}²⁻, with a Mn1...Mn1A distance of 13.364(2) Å. Each Mn atom in the bridging anionic cluster is in a 6-fold coordination of two N atoms from one chelating 2,2'-bipy and four S atoms from two chelating (As^VS₄)³⁻ anions to form a distorted (Mn₂N₄S₂) octahedral configuration. Interestingly, there exists intermolecular C–H...S hydrogen bonds, which lead to one-dimensional (1-D) chain-like structure of **1** along the *b* axis (Figure S2, Table S2). The intermolecular face-to-face π ... π stacking interactions between the aromatic rings of 2,2'-bipy with centroid–centroid distance varying from 3.695(1) to 3.881(1) Å and dihedral angles in the range 0.00(17)–8.00(12) ° lead to a three-dimensional (3-D) supramolecular network of **1** (Figure S3).

In **2**, the bridging cyclic thioarsenate anion [As^{III}₂(S₂)₂S₂]²⁻ contains two symmetry-related As³⁺ centers, each of which is double-bridged by two S₂²⁻ unit to form a chair conformation of six-membered ring with two symmetry-related S1 atoms bonding to two As atoms, respectively (Figure 2). Alternatively, the [As^{III}₂(S₂)₂S₂]²⁻ anion can also be described as two (As^{III}S₃)³⁻ trigonal-pyramids interlinked through S–S bonds. The [As^{III}₂(S₂)₂S₂]²⁻ anion bridges two [Mn(2,2'-bipy)₂(SCN)]⁺ complex cations by using its two terminal S1 atoms to yield the molecular structure of **2** with a Mn1...Mn1A separation of 10.845(2) Å. It is worthwhile to mention that although its selenium analogue [M^{III}₂(Se₂)₂Se₂]²⁻ (M = As, Sb) have been previously observed in several selenoarsenates^{5f,9} and selenoantimonates,¹⁰ the [M^{III}₂(S₂)₂S₂]²⁻ anion is rarely reported, and to our knowledge, is only known in the thioarsenate (PPh₄)₂(As₂S₆).¹¹ The intermolecular face-to-face π ... π stacking interactions between the aromatic rings of 2,2'-bipy ligands chelating to Mn1 atoms with the centroid–centroid distance varying from 3.728(1) to 3.883(1) Å and dihedral angles in the range 0.00(13)–1.87(10) ° lead to a 3-D supramolecular network of **2** (Figure S4). Structural analysis indicates that there are no significant intermolecular hydrogen bonds in the crystal structure.

The donor...acceptor distances, the donor–H...acceptor angles of the hydrogen bonds

(for **1**), and the centroid–centroid distances of the $\pi\cdots\pi$ interactions (for **1** and **2**) are comparable with the corresponding values in the literature.¹²

Up to now, several types of unsaturated TM complex cations have been found in the reported chalcogenidometalates, such as the TM complexes with a valence of +2 and four coordination sites for chalcogenide anion,¹³ a valence of +2 and two coordination sites for chalcogenide anion,¹⁴ and a valence of +2 and one coordination site for chalcogenide anion.¹⁵ However, the unsaturated TM complex cation like that in **1** and **2** with a valence of +1 and one coordination site for chalcogenide anion, to the best of our knowledge, has never been found in the reported chalcogenidometalates.

The unique structural feature of **1** is the bridging polyanion $\{[\text{Mn}(2,2'\text{-bipy})]_2(\text{As}^{\text{V}}\text{S}_4)_2\}^{2-}$ exhibiting a novel linkage mode, where two “terminal” S atoms connect with two unsaturated TM complex cations in a monodentate fashion. Similar polyanions with the general formula $\{[\text{TM}(\text{L})]_2(\text{M}'\text{Q}_4)_2\}^{q-}$ (L = bidentate chelating ligand; M' = main-group element; Q = S, Se) reported in the literature either act as a discrete anions^{14b} or coordinate with TM complex cations via two or more chalcogen atoms.¹⁶

For **2**, besides the presence of a rarely reported $[\text{M}^{\text{III}}_2(\text{S}_2)_2\text{S}_2]^{2-}$ anion, the other interesting structural feature is the cyclic thioarsenate anion bridging two TM complex cations via TM–Q bonds. Generally, the self-condensation of mononuclear $(\text{M}^{\text{III}}\text{Q}_3)^{3-}$ units leads to cyclic polymeric anions such as $(\text{M}_x\text{Q}_{2x})^{x-}$ ($x = 3$ or 4)^{10e,17} and $(\text{M}_x\text{Q}_{3x})^{2-}$ ($x = 2$) anions,¹⁰⁻¹² which usually exist as discrete anions or further condensed to extended structures. Cyclic group V chalcogenide anions acting as a bridge connecting TM ions or TM complex cations are only known for $(\text{M}_4\text{Q}_8)^{4-}$ anions^{17c,g} and a $[\text{As}(\text{S}_3)\text{S}_3]$ anion.¹⁸ Compound **2** represents the first example of the cyclic $[\text{M}^{\text{III}}_2(\text{Q}_2)_2\text{Q}_2]^{2-}$ anion bridging two TM complex cations.

3.3 TGA for **1** and **2**.

The thermal stabilities of **1** and **2** were examined by thermogravimetric analyses (TGA) in a N₂ atmosphere from 30 to 1000 °C (Figure S5). Compounds **1** and **2** have similar thermal stabilities, which reveal two-step weight losses before 1000 °C. The observed weight loss of 52.6% before 341 °C and 48.1% before 366 °C are consistent with the emission of six and four 2,2'-bipy ligands per formula for **1** and **2**, respectively (calcd 55.81% for **1** and 52.37%

for **2**). The PXRD studies indicate that MnS is one part of the TGA residues both for **1** and **2** after calcination at 1000 °C (Figure S6).

3.4 IR Spectra, Optical Spectroscopy, Photoluminescence.

In the IR spectra of **1** and **2** (Figure S7), the relatively weak bands in the region of 3087–3010 cm^{-1} correspond to the C–H vibrations of the aromatic ring hydrogen atoms, $\nu(\text{C–H})$. The bands of ring vibrations of the π -conjugated-ligand ($\nu(\text{C=C})$ and $\nu(\text{C=N})$) are observed at 1622–1400 cm^{-1} . The broad bands in the range 3457–3450 cm^{-1} are assigned to the stretching of trace water since the measurements were conducted in air. Furthermore, the IR spectra clearly show the presence of the thiocyanato groups, and also reflect their chemical environment. According to the literature,¹⁹ the $\nu(\text{CN})$ stretching of the SCN^- ligand appears from 2120 to 2080 cm^{-1} when it exhibits the N-coordinated coordination mode, whereas in compounds containing the S-coordinated SCN^- group, this value occurs in the range 2130–2100 cm^{-1} and in the case of bridging SCN^- group, this frequency is higher than 2130 cm^{-1} . The appearance of IR band at 2053 cm^{-1} for **1** and **2** indicates the presence of N-coordinated SCN^- groups rather than S-coordinated and bridging SCN^- group in their structures.

Solid state UV-vis absorption spectra of **1** and **2** calculated from the diffuse reflectance data by using the Kubela-Mulk function are plotted in Figure 3a. The optical gaps (E_g) can be estimated as 2.20 eV for **1** and 2.67 eV for **2**, which are consistent with their colors of the crystals, respectively. Compounds **1** and **2** all exhibit blue emission bands around 440 nm upon photo-excitation at 350 nm (Figure 3b), which are consistent with our previous investigation on the solid-state luminescence of other similar compounds.^{16a-c}

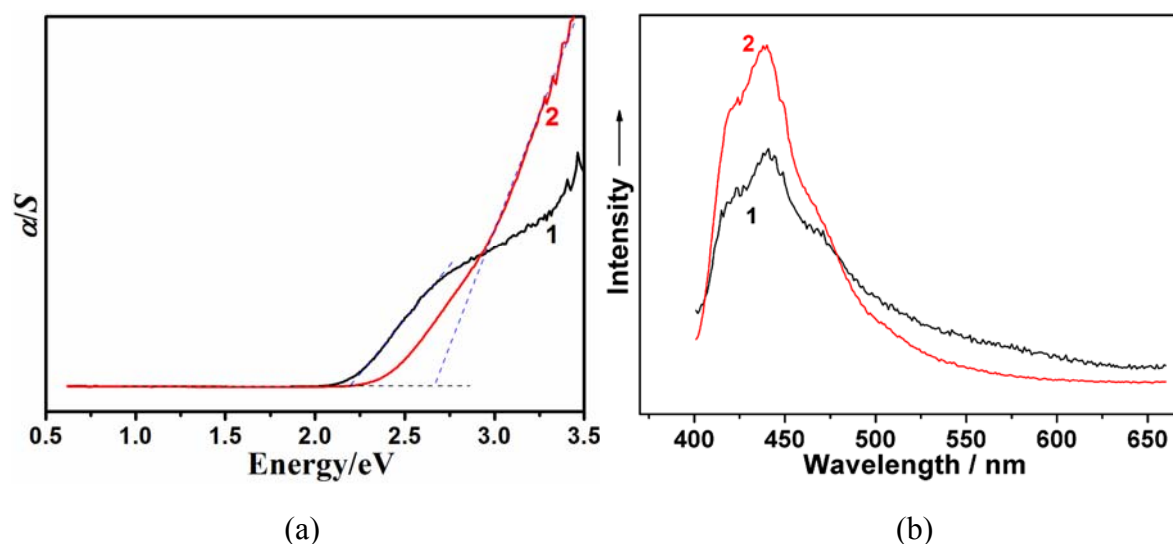


Figure 3. (a) Optical diffuse reflectance spectra for **1** and **2**. (b) Solid-state photoluminescence spectra of **1** and **2** measured at room temperature.

3.5 Magnetic Properties.

The variable-temperature magnetic susceptibility data were collected for **1** at an applied dc field of 1000 Oe in the 2–300 K temperature range. The $\chi_M T$ vs T and χ_M vs T plots for **1** are shown in Figure 4 (χ_M is the molar magnetic susceptibility per formula). At 300 K, the $\chi_M T$ value is $16.946 \text{ cm}^3 \cdot \text{K} \cdot \text{mol}^{-1}$, which is in agreement with the value of $17.500 \text{ cm}^3 \cdot \text{K} \cdot \text{mol}^{-1}$ expected for four high-spin Mn^{2+} ions with $S = 5/2$ and $g = 2.00$. Upon cooling, $\chi_M T$ decreases monotonically and reaches a value of $5.548 \text{ cm}^3 \cdot \text{K} \cdot \text{mol}^{-1}$ at 2 K. Meanwhile, χ_M gradually increases from $0.057 \text{ cm}^3 \cdot \text{mol}^{-1}$ at 300 K to a value of $2.788 \text{ cm}^3 \cdot \text{mol}^{-1}$ at about 2 K. This character suggests the dominant antiferromagnetic interaction between the Mn^{II} centers in **1**. The $1/\chi_M$ vs T curve above 50 K obeys the Curie-Weiss law with $C = 17.83 \text{ cm}^3 \cdot \text{K} \cdot \text{mol}^{-1}$ and $\theta = -17.75 \text{ K}$ (Figure 4, insert). The negative θ value further confirms the antiferromagnetic coupling among the Mn^{2+} ions.

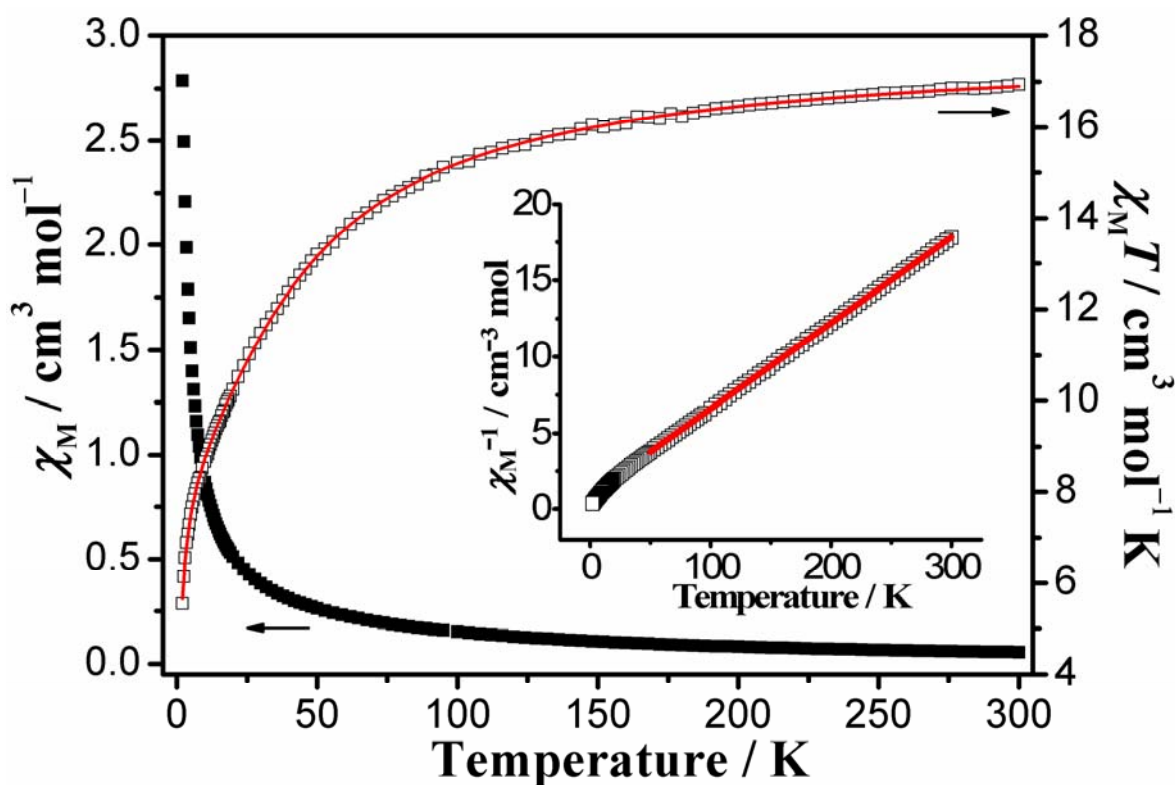


Figure 4. Temperature dependence of χ_M and $\chi_M T$ for **1**. The solid line shows the best fitting result by using the theoretical model as shown in equation (3). Insert: the temperature dependence of χ_M^{-1} for **1** with the solid line representing the fit of the Curie-Weiss law.

To quantitatively analyze the magnetic behavior of **1**, we assume that the magnetic coupling of **1** is dominated by the exchange between the $[\text{Mn}2]_2$ dimers and the Mn1 ions are treated as paramagnetic ions based on the structural analysis, in which the Mn2...Mn2A separation of 3.769(1) Å bridged by two chelating $(\text{As}^{\text{V}}\text{S}_4)^{3-}$ anions is much shorter than the Mn1...Mn2 and Mn1...Mn2A distances (7.084(1) and 6.798(1) Å, respectively) connected by –S–As–S– bridges. Accordingly, the molar magnetic susceptibility of **1** can be written as²⁰

$$\chi_{\text{tetra}} = \chi_{bi} + \frac{2Ng^2\beta^2 S(S+1)}{3KT} \quad (1)$$

where the χ_{bi} is for the $[\text{Mn}2]_2$ dimer as shown in equation (2)

$$\chi_{bi} = \frac{2Ng^2\beta^2}{KT} \frac{A}{B} \quad (2)$$

with $A = e^{J/KT} + 5e^{3J/KT} + 14e^{6J/KT} + 30e^{10J/KT} + 55e^{15J/KT}$, $B = 1 + 3e^{J/KT} + 5e^{3J/KT} + 7e^{6J/KT} + 9e^{10J/KT} + 11e^{15J/KT}$, and the latter is the contribution of two paramagnetic Mn1 ions. Moreover,

taking into consideration of the intermolecular interactions (zJ'), the magnetic data can be well fitted using the following expression

$$\chi = \frac{\chi_{tetra}}{1 - (2zJ'/Ng^2\beta^2)\chi_{tetra}} \quad (3)$$

The best-fitting parameters obtained in the whole temperature range are $g = 2.02(1)$, $J = -3.17(2) \text{ cm}^{-1}$, $zJ' = -0.07(1) \text{ cm}^{-1}$ and $R = 6.50 \times 10^{-6}$. The negative J value confirms the antiferromagnetic coupling between the Mn²⁺ ions bridged by two chelating (As^VS₄)³⁻ anions.

The magnetic susceptibility of **2** has been measured under a constant magnetic field of 5000 Oe and the data are presented as plots of $\chi_M T$ vs T and χ_M vs T in Figure 5. At 300 K, the $\chi_M T$ product of $8.867 \text{ cm}^3 \cdot \text{K} \cdot \text{mol}^{-1}$ is comparable with the spin-only one expected for two isolated Mn²⁺ ions ($8.750 \text{ cm}^3 \cdot \text{K} \cdot \text{mol}^{-1}$). Upon cooling, the $\chi_M T$ product remains nearly constant in the temperature range 300–50 K, and then gradually decreases to a value of $7.267 \text{ cm}^3 \cdot \text{K} \cdot \text{mol}^{-1}$ at 2 K, which indicates the paramagnetic behavior for **2**. The inverse magnetic susceptibility data above 50 K were fitted by the Curie-Weiss law $1/\chi_M = (T - \theta)/C$ with parameters $C = 8.85 \text{ cm}^3 \cdot \text{K} \cdot \text{mol}^{-1}$ and $\theta = -0.35 \text{ K}$ (Figure 5, insert). The very small negative θ value indicates the presence of negligible weak antiferromagnetic interactions between Mn²⁺ ions in **2**.

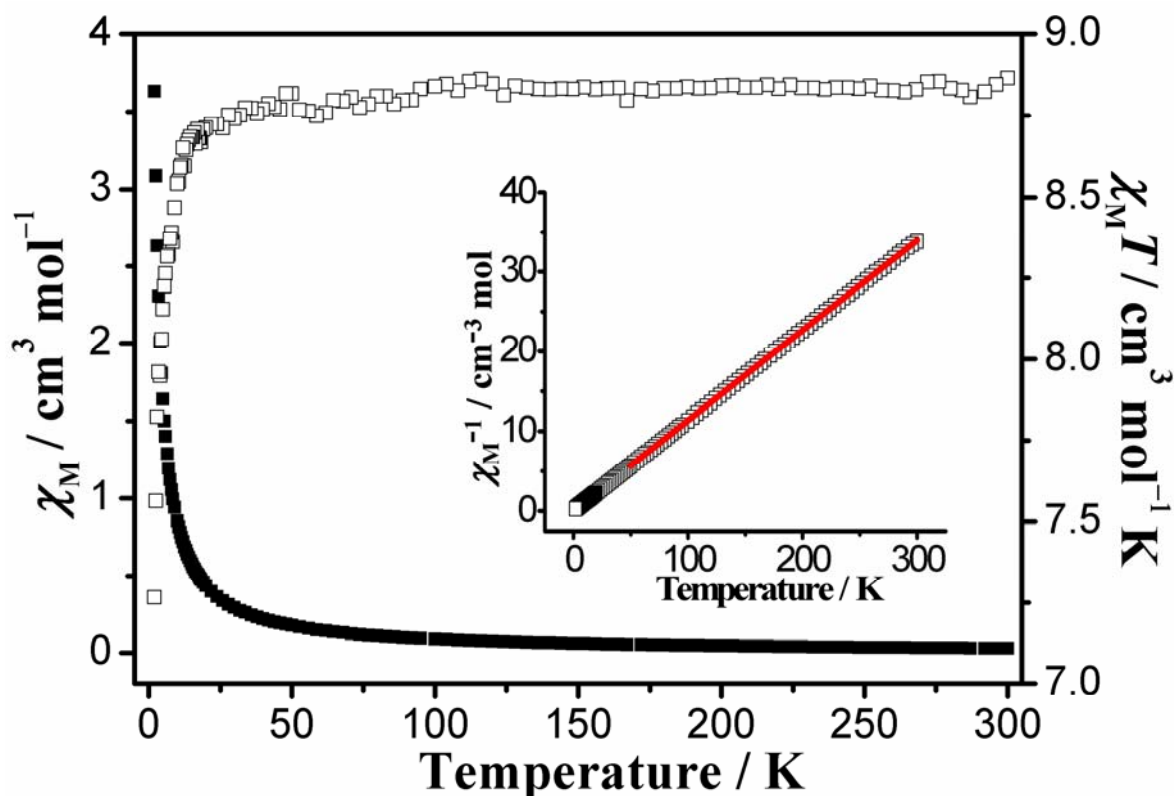


Figure 5. Temperature dependence of χ_M and $\chi_M T$ for **2**. Insert: the temperature dependence of χ_M^{-1} for **2**; the solid line represents the fit of the Curie-Weiss law.

The thioarsenate anions and their linkage modes with paramagnetic Mn^{2+} ions determine the type and the strength of the magnetic exchange coupling (Figure 6, Table 2). In **1–2**, the shortest intramolecular $\text{Mn}\cdots\text{Mn}$ distances are in the range of 3.769(1)–10.845(2) Å, which are too long for significant direct magnetic exchanges. Consequently, the magnetic exchange in **1–2** is of superexchange type. Meanwhile, the strengths of the superexchange interactions are influenced by the $\text{Mn}\cdots\text{Mn}$ distances. In **1**, the tetrahedral $(\text{AsS}_4)^{3-}$ anions bridge two Mn^{2+} ions via two $\mu_3\text{-S}$ atoms with a shorter $\text{Mn}\cdots\text{Mn}$ distance of 3.769(1) Å (compared with that in **2**), which causes a stronger antiferromagnetic couplings, $J = -3.17(2) \text{ cm}^{-1}$ and $\theta = -17.75 \text{ K}$. In **2**, a cyclic thioarsenate anion $[\text{As}^{\text{III}}_2(\text{S}_2)_2\text{S}_2]^{2-}$ separates the intramolecular Mn ions with a longer $\text{Mn}\cdots\text{Mn}$ distance of 10.845(2) Å, leading to a weaker antiferromagnetic couplings, $\theta = -0.35 \text{ K}$. For **1** and **2**, the strengths of the antiferromagnetic interactions are comparable with the reported compounds with similar bridges of magnetic interactions, and $\text{Mn}\cdots\text{Mn}$ distances.^{12,20c}

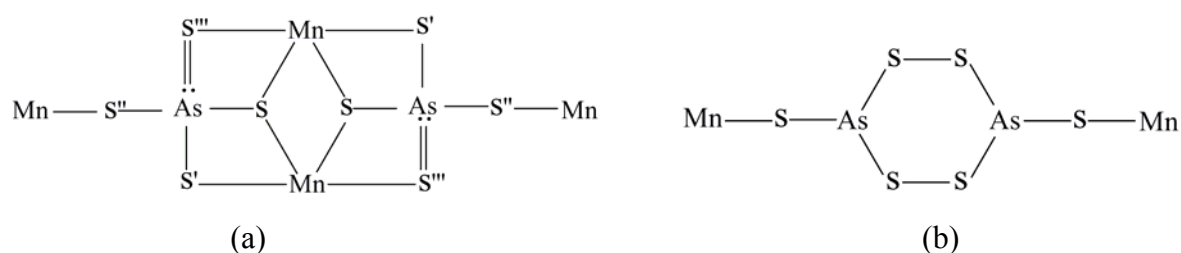


Figure 6. The linkage modes of the tetrahedral $(\text{AsS}_4)^{3-}$ anion in **1** (a), and the cyclic thioarsenate anion $[\text{As}^{\text{III}}_2(\text{S}_2)_2\text{S}_2]^{2-}$ in **2** (b).

Table 2. Summary of the Magnetic Exchange Pathways, Minimum Mn...Mn Distances and Magnetic Parameters for **1–2**.

	1	2
bridging units	$(\text{AsS}_4)^{4-}$	$[\text{As}^{\text{III}}_2(\text{S}_2)_2\text{S}_2]^{2-}$
possible magnetic exchange pathways	$-(\mu_3\text{-S})_2-$	$-\text{S-As-(S-S)}_2\text{-As-S-}$
$\angle \text{Mn-S-Mn}$ [$^\circ$]	89.92(3)	/
Mn...Mn [\AA] ^a	3.769(1)	10.845(2)
θ [K]	-17.75	-0.35
J [cm^{-1}]	-3.17(2)	/
zJ' [cm^{-1}]	-0.07(1)	/

^a The intramolecular Mn...Mn distance.

4. Conclusion

In this work, by selecting SCN^- as an anionic second ligand to modify the number of the coordinate site and the charge of the TM complex cation simultaneously, an unsaturated TM complex cation, $[\text{Mn}(2,2'\text{-bipy})_2(\text{SCN})]^+$ was formed *in-situ*, which further direct the formation of two novel chalcogenidometalates $\{[\text{Mn}(2,2'\text{-bipy})_2(\text{SCN})][\text{Mn}(2,2'\text{-bipy})](\text{As}^{\text{V}}\text{S}_4)\}_2$ and $\{[\text{Mn}(2,2'\text{-bipy})_2(\text{SCN})]_2(\text{As}^{\text{III}}_2\text{S}_6)\}$. The two compounds exhibit wide optical gaps of 2.20 and 2.67 eV, respectively and show the presence of antiferromagnetic interactions between Mn^{II} centers. The approach to obtain new unstaturated complex cations shown here differs from the traditional methods and may open up a new way to synthesize novel chalcogenidometalates. Work in this direction is underway

in our laboratory.

5. Acknowledgement

We gratefully acknowledge the financial support by the NSF of China (21221001, 21201080, 21103188), the NSF of Fujian and Shandong Province (2010H0022, 2011J06006, ZR2012BQ011).

6. Supporting Information.

Crystallographic data (CIFs; CCDC reference numbers 819897 for **1** and 819898 for **2**, additional structural figures, TGA curves, IR spectra, and PXRD patterns. This materials is available free of charge via the Internet at <http://pubs.acs.org>.

References

- (1) (a) G. W. Drake, J. W. Kolis, *Coord. Chem. Rev.* 1994, **137**, 131; (b) J. Li, Z. Chen, R.-J. Wang, D. M. Proserpio, *Coord. Chem. Rev.* 1999, **190-192**, 707. (c) J. Zhou, J. Dai, G.-Q. Bian, C.-Y. Li, *Coord. Chem. Rev.* 2009, **253**, 1221. (d) B. Seidlhofer, N. Pienack, W. Bensch, *Z. Naturforsch.* 2010, **65**, 937. (e) W. Su, X. Huang, J. Li, H. Fu, *J. Am. Chem. Soc.* 2002, **124**, 12944. (f) W. S. Sheldrick, *J. Chem. Soc., Dalton Trans.* 2000, 3041. (g) S. Dehnen, M. Melullis, *Coord. Chem. Rev.* 2007, **251**, 1259. (h) M. Yuan, D. B. Mitzi, *Dalton Trans.* 2009, 6078. (i) O. M. Yaghi, Z. Sun, D. A. Richardson, T. L. Groy, *J. Am. Chem. Soc.* 1994, **116**, 807. (j) J. B. Parise, K. M. Tan, *Chem. Commun.* 1996, 1687. (k) M. J. MacLachlan, N. Coombs, G. A. Ozin, *Nature* 1999, **397**, 681. (l) A. Shah, P. Torres, R. Tscherner, N. Wyrsh, H. Keppner, *Science* 1999, **285**, 692. (m) T. K. Bera, J.-H. Song, A. J. Freeman, J. I. Jang, J. B. Ketterson, M. G. Kanatzidis, *Angew. Chem., Int. Ed.* 2008, **47**, 7828. (n) N. Ding, M. G. Kanatzidis, *Nat. Chem.* 2010, **2**, 187. (o) M.-L. Feng, D.-N. Kong, Z.-L. Xie, X.-Y. Huang, *Angew. Chem., Int. Ed.* 2008, **47**, 8623. (p) P. Feng, X. Bu, N. Zheng, *Acc. Chem. Res.* 2005, **38**, 293. (q) N. Zheng, H. Lu, X. Bu, P. Feng, *J. Am. Chem. Soc.* 2006, **128**, 4528. (r) Q. Zhang, Y. Liu, X. Bu, T. Wu, P. Feng, *Angew. Chem., Int. Ed.* 2008, **47**, 113.
- (2) in this paper, "unsaturated metal complex cations " means after the coordination with

organic ligands, the metal ion doesn't reach its highest coordination number and still has the ability to coordinate with chalcogenide anions.

- (3) (a) W. Bensch, C. Näther, M. Schur, *Chem. Commun.* 1997, 1773. (b) Z. Rejai, H. Lühmann, C. Näther, R. K. Kremer, W. Bensch, *Inorg. Chem.* 2010, **49**, 1651. (c) J. Zhou, G.-Q. Bian, J. Dai, Y. Zhang, A.-B. Tang, Q.-Y. Zhu, *Inorg. Chem.* 2007, **46**, 1541. (d) Q. Zhang, X. Bu, Z. Lin, M. Biasini, W. P. Beyermann, P. Feng, *Inorg. Chem.* 2007, **46**, 7262. (e) M. J. Manos, M. G. Kanatzidis, *Inorg. Chem.* 2009, **48**, 4658. (f) M.-L. Feng, D. Ye, X.-Y. Huang, *Inorg. Chem.* 2009, **48**, 8060. (g) J.-F. Chen, Q.-Y. Jin, Y.-L. Pan, Y. Zhang, D.-X. Jia, *Chem. Commun.* 2009, 7212. (h) Z. Wang, H. Zhang, C. Wang, *Inorg. Chem.* 2009, **48**, 8180. (i) J. Zhou, L. An, X. Liu, H. Zou, F. Hu, C. Liu, *Chem. Commun.* 2012, **48**, 2537.
- (4) (a) M. Zhang, T.-L. Sheng, X.-H. Huang, R.-B. Fu, X. Wang, S.-M. Hu, S.-C. Xiang, X.-T. Wu, *Eur. J. Inorg. Chem.* 2007, 1606. (b) D. Jia, Q. Jin, J. Chen, Y. Pan, Y. Zhang, *Inorg. Chem.* 2009, **48**, 8286. (c) G.-N. Liu, G.-C. Guo, M.-S. Wang, L.-Z. Cai, J.-S. Huang, *J. Mol. Struct.* 2010, **983**, 104.
- (5) (a) J. Zhou, Y. Zhang, G.-Q. Bian, Q.-Y. Zhu, C.-Y. Li, J. Dai, *Cryst. Growth Des.* 2007, **7**, 1889. (b) H. Lühmann, Z. Rejai, K. Möller, P. Leisner, M. E. Ordolff, C. Näther, W. Bensch, *Z. Anorg. Allg. Chem.* 2008, **634**, 1687. (c) J. Wang, Y. Pan, J. Chen, J. Gu, Y. Zhang, D. Jia, *Dalton Trans.* 2010, **39**, 7066. (d) J. Zhao, J. Liang, Y. Pan, Y. Zhang, D. Jia, *J. Solid State Chem.* 2011, **184**, 1451. (e) J. Liang, J. Chen, J. Zhao, Y. Pan, Y. Zhang, D. Jia, *Z. Anorg. Allg. Chem.* 2011, **637**, 445. (f) D. Jia, J. Zhao, Y. Pan, W. Tang, B. Wu, Y. Zhang, *Inorg. Chem.* 2011, **50**, 7195.
- (6) W. M. Wendlandt, H. G. Hecht, *Reflectance Spectroscopy*; Interscience: New York, 1966.
- (7) *CrystalStructure*; Version 3.10; Rigaku Corp. and Rigaku/MSK: Tokyo, Japan, 2002.
- (8) *SHELXTL Reference manual, Version 5*; Siemens Energy & Automation Inc.: Madison, WI, 1994.
- (9) (a) C. H. E. Belin, M. M. Charbonnel, *Inorg. Chem.* 1982, **21**, 2504. (b) M. A. Ansari, J. A. Ibers, S. C. Oneal, W. T. Pennington, J. W. Kolis, *Polyhedron* 1992, **11**, 1877. (c) W. Czado, U. Müller, *Z. Anorg. Allg. Chem.* 1998, **624**, 239. (d) D. M. Smith, M. A. Pell, J. A. Ibers, *Inorg. Chem.* 1998, **37**, 2340. (e) M.-L. Fu, G.-C. Guo, X. Liu, B. Liu, L.-Z. Cai,

- J.-S. Huang, *Inorg. Chem. Commun.* 2005, **8**, 18. (f) T. Van Almsick, W. S. Sheldrick, *Acta Crystallogr., Sect. E: Struct. Rep. Online* 2005, **61**, M2431. (g) A. Kromm, W. S. Sheldrick, *Acta Crystallogr., Sect. E: Struct. Rep. Online* 2007, **63**, M581.
- (10) D. M. Smith, C. W. Park, J. A. Ibers, *Inorg. Chem.* 1997, **36**, 3798.
- (11) K. Wendel, U. Müller, *Z. Anorg. Allg. Chem.* 1995, **621**, 979.
- (12) G.-N. Liu, G.-C. Guo, F. Chen, S.-H. Wang, J. Sun, J.-S. Huang, *Inorg. Chem.* 2012, **51**, 472.
- (13)(a) M. Schur, W. Bensch, *Z. Naturforsch.* 2002, **57**, 1. (b) M. Melullis, M. K. Brandmayer, S. Dehnen, *Z. Anorg. Allg. Chem.* 2006, **632**, 64. (c) G.-N. Liu, X.-M. Jiang, M.-F. Wu, G.-E. Wang, G.-C. Guo, J.-S. Huang, *Inorg. Chem.* 2011, **50**, 5740.
- (14)(a) R. Stähler, W. Bensch, *J. Chem. Soc., Dalton Trans.* 2001, 2518. (b) M. Schaefer, R. Stähler, W. R. Kiebach, C. Näther, W. Bensch, *Z. Anorg. Allg. Chem.* 2004, **630**, 1816. (c) A. Kromm, W. S. Sheldrick, *Z. Anorg. Allg. Chem.* 2008, **634**, 225. (d) Y. Pan, Q. Jin, J. Chen, Y. Zhang, D. Jia, *Inorg. Chem.* 2009, **48**, 5412.
- (15)(a) J. Zhou, G.-Q. Bian, Y. Zhang, Q.-Y. Zhu, C.-Y. Li, J. Dai, *Inorg. Chem.* 2007, **46**, 6347. (b) J. Zhou, Y. Zhang, G.-Q. Bian, C.-Y. Li, X.-X. Chen, J. Dai, *Cryst. Growth Des.* 2008, **8**, 2235. (c) N. Pienack, S. Lehmann, H. Lühmann, M. El-Madani, C. Näther, W. Bensch, *Z. Anorg. Allg. Chem.* 2008, **634**, 2323.
- (16)(a) M.-L. Fu, G.-C. Guo, X. Liu, W.-T. Chen, B. Liu, J.-S. Huang, *Inorg. Chem.* 2006, **45**, 5793. (b) G.-N. Liu, G.-C. Guo, F. Chen, S.-P. Guo, X.-M. Jiang, C. Yang, M.-S. Wang, M. F. Wu, J.-S. Huang, *CrystEngComm* 2010, **12**, 4035. (c) G.-N. Liu, X.-M. Jiang, M.-F. Wu, G.-E. Wang, G.-C. Guo, J.-S. Huang, *Inorg. Chem.* 2011, **50**, 5740. (d) X. Wang, T.-L. Sheng, S.-M. Hu, R.-B. Fu, J.-S. Chen, X.-T. Wu, *J. Solid State Chem.* 2009, **182**, 913.
- (17)(a) W. S. Sheldrick, J. Kaub, *Z. Naturforsch.* 1985, **40b**, 19. (b) W. S. Sheldrick, J. Kaub, *Z. Naturforsch.* 1985, **40b**, 1020. (c) A. Kromm, W. S. Sheldrick, *Z. Anorg. Allg. Chem.* 2008, **634**, 2948. (d) J.-H. Chou, M. G. Kanatzidis, *Chem. Mater.* 1995, **7**, 5. (e) M. Wachhold, M. G. Kanatzidis, *Inorg. Chem.* 1999, **38**, 4178. (f) W. Bensch, C. Näther, R. Stähler, *Chem. Commun.* 2001, 477. (g) R. Kiebach, W. Bensch, R. D. Hoffmann, R. Pöttgen, *Z. Anorg. Allg. Chem.* 2003, **629**, 532. (h) Y. D. Wu, W. Bensch, *Inorg. Chem.* 2009, **48**, 2729. (i) E. Quiroga-Gonzalez, C. Näther, W. Bensch, *Solid State Sci.* 2010, **12**,

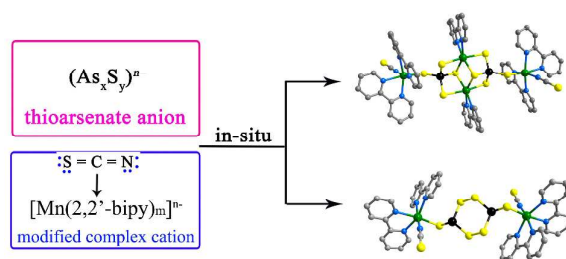
1235.

(18) A. Kromm, W. S. Sheldrick, *Z. Anorg. Allg. Chem.* 2008, **634**, 121.

(19) K. B. Yatsimir, *Pure Appl. Chem.* 1977, **49**, 115.

(20) (a) M. E. Fisher, *Am. J. Phys.* 1964, **32**, 343-346; (b) C. J. Oconnor, *Prog. Inorg. Chem.* 1982, **29**, 203-283. (c) Y.-B. Lu, M.-S. Wang, W.-W. Zhou, G. Xu, G.-C. Guo, J.-S. Huang, *Inorg. Chem.* 2008, **47**, 8935.

Table of Contents



This work demonstrates that introducing an anionic second ligand to modify transition metal complex cations can direct the formation of novel chalcogenidometalates.